Atherosclerosis 315 (2020) 1–9

Contents lists available at ScienceDirect

Atherosclerosis

journal homepage: www.elsevier.com/locate/atherosclerosis

Regulation of intestinal LDLR by the LXR-IDOL axis

Nienke M. van Loon [2], Suzanne A.E. van Wouw [2], Roelof Ottenhoff, Jessica K. Nelson [1], Jenina Kingma, Saskia Scheij, Martina Moeton, Noam Zelcer [*]

Department of Medical Biochemistry, Amsterdam UMC, Amsterdam Cardiovascular Sciences and Gastroenterology and Metabolism, University of Amsterdam, Meibergdreef 9, 1105AZ, Amsterdam, the Netherlands

ARTICLE INFO

Keywords:
Cholesterol metabolism
LDLR
IDOL
LXR
TICE

ABSTRACT

Background and aims: Cholesterol metabolism is tightly regulated by transcriptional and post-transcriptional mechanisms. Accordingly, dysregulation of cholesterol metabolism is a major risk factor for the development of coronary artery disease and associated complications. In recent years, it has become apparent that next to the liver, the intestine plays a key role in systemic cholesterol metabolism by governing cholesterol absorption, secretion, and incorporation into lipoprotein particles. We have previously demonstrated that the Liver X receptor (LXR)-regulated E3 ubiquitin ligase inducible degrader of LDLR (IDOL) is a regulator of cholesterol uptake owing to its ability to promote the ubiquitylation of the low-density lipoprotein receptor (LDLR). However, whether the LXR-IDOL-LDLR axis regulates the LDLR in the intestine and whether this influences intestinal cholesterol homeostasis is not known.

Methods: In this study, we evaluated the role of the LXR-IDOL-LDLR axis in enterocyte cell models and in primary enterocytes isolated from *Idol*$^{(-/-)}$ and wild type mice. Furthermore, we studied the regulation of intestinal LDLR in *Idol*$^{(-/-)}$ and in wild type mice treated with the LXR agonist GW3965. Finally, we assessed ezetimibe-induced *trans*-intestinal cholesterol efflux in *Idol*$^{(-/-)}$ mice.

Results: We show that in a wide range of intestinal cell lines LXR activation decreases LDLR protein abundance, cell surface occupancy, and LDL uptake in an IDOL-dependent manner. Similarly, we find that pharmacological dosing of C57BL6/N mice with the LXR agonist GW3965 increases *Idol* expression across the intestine with a concomitant reduction in Ldlr protein. Conversely, primary enterocytes isolated from *Idol*$^{(-/-)}$ mice have elevated Ldlr. To test whether these changes contribute to *trans*-intestinal cholesterol efflux, we measured fecal cholesterol in mice following ezetimibe dosing, but found no differences between *Idol*$^{(-/-)}$ and control mice in this setting.

Conclusions: In conclusion, our study establishes that the LXR-IDOL-LDLR axis is active in the intestine and is part of the molecular circuitry that maintains cholesterol homeostasis in enterocytes.

1. Introduction

Cholesterol is an essential component of eukaryotic cell membranes and a precursor for a variety of bioactive molecules. However, increased intracellular concentrations can be cytotoxic and elevated levels of atherogenic lipoproteins are an established risk factor for the development of atherosclerosis. It follows that understanding the basic mechanisms that govern cholesterol metabolism is a prerequisite for further development of therapeutic strategies to treat dyslipidemia and improve lipid-lowering strategies.

The liver and intestines play a prominent role in governing systemic cholesterol metabolism. Next to dietary uptake via the intestinal cholesterol transporter NPC1L1 [1], cholesterol can be synthesized in the liver and intestines, and both organs significantly contribute to the plasma pool of cholesterol in humans [2,3]. The relative contribution of the liver and intestine to total synthesized cholesterol differs substantially between species. In mice, 21–38% of synthesized cholesterol has been reported to originate from the liver, and 12–24% from the small

* Corresponding author. Department of Medical Biochemistry Academic Medical Center of the University of Amsterdam, Meibergdreef 15, 1105AZ, Amsterdam, the Netherlands.
E-mail address: n.zelcer@amsterdamumc.nl (N. Zelcer).
[1] Current affiliation: Adult Stem Cell Laboratory, The Francis Crick Institute, 1 Midland Road, London NW1 1AT, United Kingdom.
[2] These authors contributed equally to the work.

https://doi.org/10.1016/j.atherosclerosis.2020.10.898
Received 15 June 2020; Received in revised form 8 October 2020; Accepted 30 October 2020
Available online 9 November 2020

intestines, with pronounced variation between different mouse strains and diets [4]. Conversely, cholesterol is classically thought to be secreted from the human body into the feces through the coordinated action of hepatic transporters that results in biliary secretion of cholesterol directly, or of bile acids, which are synthesized from cholesterol in the liver, in a process collectively referred to as reversed cholesterol transport (RCT) [1,4,5]. An alternative pathway for cholesterol loss referred to as trans intestinal cholesterol excretion (TICE) has been proposed [4,6]. This process can be stimulated by ezetimibe [7,8], plant sterols [9,10] or with agonists stimulating Farnesoid X receptors [11], Liver X receptors (LXRs) [12,13] or peroxisome-proliferator-activated-receptor-delta [14], as well as through modulation of hepatic cholesterol metabolism [15,16]. TICE is thought to involve the transcellular trafficking of lipoproteins through the enterocyte layer and subsequent deposition of cholesterol directly into the intestinal lumen [4,6]. Despite significant efforts, the identity of the transported lipoprotein as well as the basolateral uptake receptor(s) are still unclear [17]. As in mice, TICE has been also reported in humans and is estimated to account for up to 30–44% of daily cholesterol loss [8, 18–20].

The ability of ezetimibe to stimulate TICE and reduce circulating cholesterol levels has been, at large, attributed to the ability of the drug to attenuate intestinal cholesterol absorption [21]. Intriguingly, a recent study demonstrated that a consequence of ezetimibe treatment in enterocytes is a dramatic increase in the level of the low-density lipoprotein receptor (LDLR) in the basolateral membrane, and a decrease in expression of the E3 ubiquitin ligase inducible degrader of LDLR (IDOL) [22]. While these transcriptional changes can be explained by sterol-depletion of enterocytes that activates signaling by the sterol regulatory element binding proteins (SREBPs), and concomitantly decreases LXRs signaling (reviewed in [23–25]), it may also suggest involvement of Idol and LDLR in ezetimibe-stimulated TICE. Idol is an LXR-regulated E3 ubiquitin ligase that promotes the ubiquitylation and subsequent degradation of the LDLR and its related family members, the very low density lipoprotein receptor and ApoE receptor 2 [26,27]. In line with the regulation of these receptors, we and others have shown that Idol plays a prominent role in a wide range of (patho)physiological conditions, including regulation of systemic lipid and energy metabolism [28–30], Alzheimer's disease [31], neuronal function [32,33] and viral entry [34], as reviewed in [35]. Moreover, genetic variation in the *IDOL* locus has been associated with circulating cholesterol levels in humans [36], and we and others have reported *IDOL* variants that influence cholesterol levels in human carriers [37–39]. Collectively, these studies suggest that IDOL plays an important role in human lipoprotein metabolism. IDOL is broadly expressed in the intestinal tract, but whether the LXR-IDOL-LDLR axis is active in the intestine and contributes to TICE is not known.

2. Materials and methods

2.1. Cell culture

The human colon-derived enterocyte-like cell lines HCT116, HT29 and SW480 were obtained from ATCC and grown at 37 °C and 5% CO_2 in Dulbecco's Modified Eagle Medium (DMEM) (Gibco) supplemented with 10% fetal bovine serum (FBS), penicillin (100 units/mL) and streptomycin (100 μg/mL). To deplete cellular sterols, cells were washed twice with PBS and culture medium was replaced with DMEM containing 10% lipoprotein deficient serum (as described previously [40]), supplemented with 100 μM mevalonate (Sigma) and 2.5 μg/mL simvastatin (Calbiochem). To stimulate LXR-dependent signaling, the pharmacological agonist GW3965 (Sigma), dissolved in DMSO, was added to the culture media at a final concentration of 2 μM. As control, in these experiments a similar volume of vehicle was added to the culture media.

2.2. Transfection of cells

HCT116 cells were detached by TripLE (Life Technologies) and diluted in DMEM supplemented with 10% FBS, but lacking penicillin or streptomycin. Cells were reverse-transfected upon plating with siRNAs using Lipofectamine RNAiMAX (Life Technologies). Briefly, cells were transfected with 30 nM of the on-target plus smartpool Idol siRNA (si*IDOL*) or non-targeting control siRNA (siNT) (Dharmacon) prepared in optiMEM. Subsequently, 16 h post transfection, cells were washed with PBS and cultured for an additional 24 h in sterol-depletion media in the presence or absence of GW3965 as indicated.

2.3. Immunoblot analysis

Total cell lysates were prepared in radio-immunoprecipitation assay (RIPA) buffer (Boston Biochem) supplemented with phenylmethylsulfonyl fluoride (Sigma) and protease inhibitors (Roche) by agitation at 4 °C for 30 min. Subsequently, samples were cleared by centrifugation at 4 °C at 10,000*g* for 10 min. Whole tissue lysates were prepared by lysing sections of jejunum and ileum in RIPA buffer (Biochem) supplemented with phenylmethylsulfonyl fluoride (Sigma) and protease inhibitors (Roche). Subsequently, tissue samples were incubated at 4 °C for 60 min with agitation, and cleared by centrifugation as above. Protein concentration was determined using a BCA assay (ThermoFisher) following the manufacturers' protocol, and an equal amount was loaded for analysis. Samples were separated on NuPAGE Novex 4–12% Bis-Tris gels (ThermoFisher) and transferred unto nitrocellulose membranes, blocked in 5% milk (Elk) in PBS supplemented with Tween and subsequently probed with primary antibodies. The primary antibodies used in this study are mouse anti Actin (1:3000, MAB1501, Merck Millipore) and rabbit anti LDLR (1:1000, 3839, Bio-Vision and 1:1000, Cayman, 10,007,665). Secondary HRP-conjugated antibodies (A28177 & A27036, Invitrogen) were used and visualized with chemiluminescence on a Fuji LAS4000 (GE Healthcare).

2.4. Quantitative PCR

RNA was isolated from cells using the Direct-zol RNA miniprep kit (Zymo Research), and from tissue by manual Trireagent (Sigma) extraction following the manufacturer's protocol. cDNA was generated using the iScript reverse transcription reagent (BioRad). SensiFAST SYBRgreen (Bioline) was used for real-time quantitative PCR (RT-qPCR). Measurements were performed on a LightCycler 480 II system (Roche) and gene expression was normalized to the expression level of 36b4 for cell lines and *Rplp0/Rpl13* for murine samples. Primer sequences are shown in Supplementary Table 1.

2.5. Surface LDLR assay

To determine the level of surface LDLR cells were treated as indicated in the figure legends, dissociated using TrypLE (Life Technologies), and washed once with FACS buffer (2 mM EDTA, 0.5% BSA in PBS). Subsequently, cells were stained with an allophycocyanin (APC)-conjugated mouse anti-human LDLR antibody (R&D; #FAB2148A, 10 μL/1 × 10^6 cells) on ice protected from light. Cells were then washed three times with FACS buffer and fluorescence was directly analyzed on a CytoFLEX Flow cytometer (Beckman Coulter). Intact cells were gated by standard FSC *vs* SSC gating. Relative surface LDLR levels were calculated from median values after correction for background signal.

2.6. LDL uptake assay

Cellular LDL uptake was measured as previously reported by Loregger et al. [41]. Briefly, HCT116 were plated and sterol-depleted for 16 h. Subsequently, cells were washed with PBS and incubated for 1 h with 5 μg/mL Dylight-488-labelled LDL (kind gift of Dr. Geesje Dallinga-Thie,

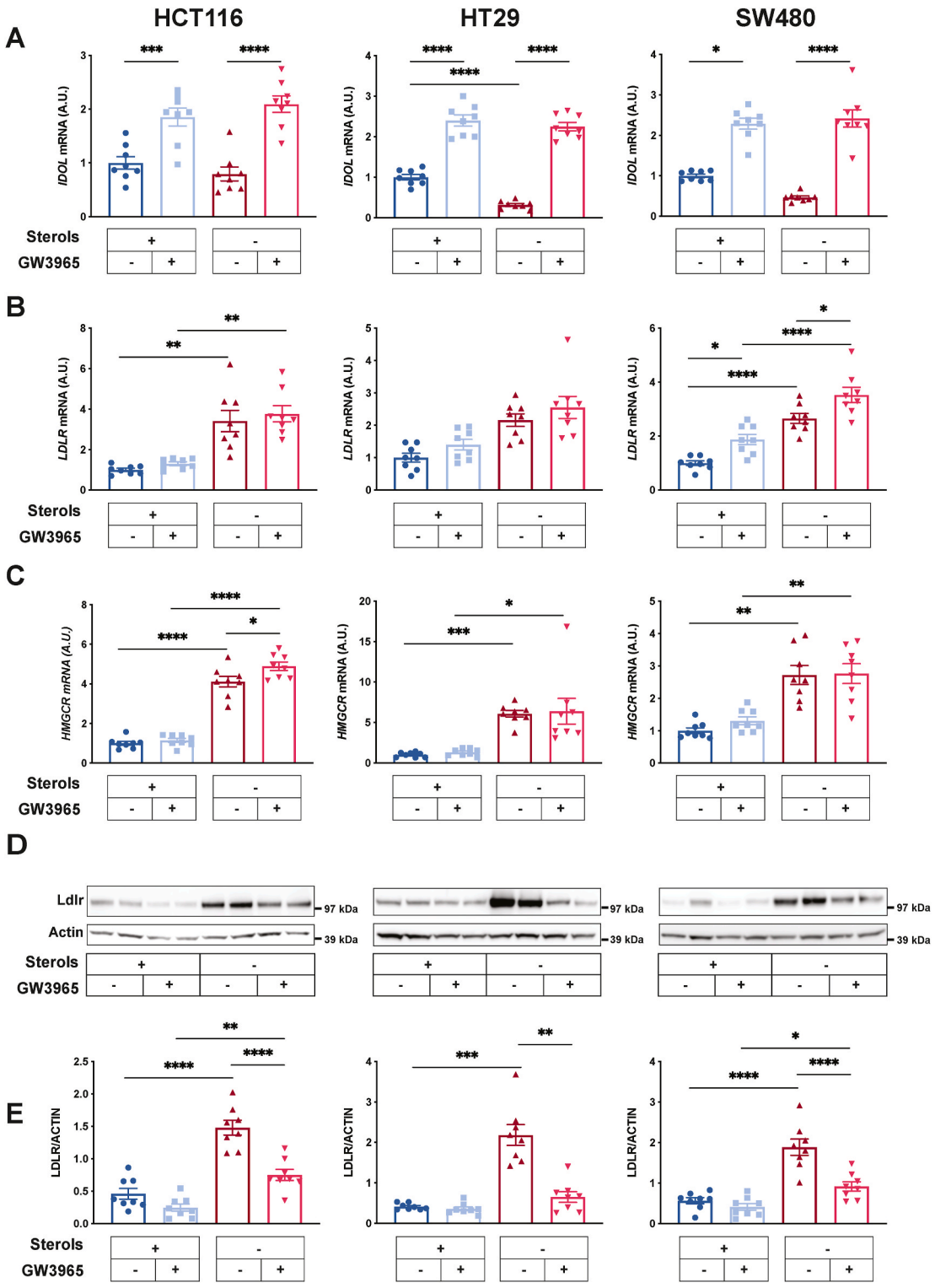

Fig. 1. The LXR-IDOL-LDLR axis is active in human enterocyte cell lines.
HCT116 (left panel), HT29 (center panel) and SW480 (right panel) cells were cultured in complete or sterol-depleted media (indicated with sterols +/−), in the presence or absence of 2 μM of the LXR agonist GW3965. The expression of (A) *IDOL*, (B) *HMGCR*, and (C) *LDLR* was determined by qPCR as shown. (D) Total cell lysates were prepared from cells cultured as described in (A) and a representative immunoblot is shown. (E) Quantification of the intensity of the LDLR normalized to ACTIN. Each bar and error represent the mean ± SEM. Statistical differences between groups were evaluated with a one way ANOVA as described in the Materials and methods section. *$p < 0.05$, **$p < 0.01$, ***$p < 0.001$, ****$p < 0.0001$.

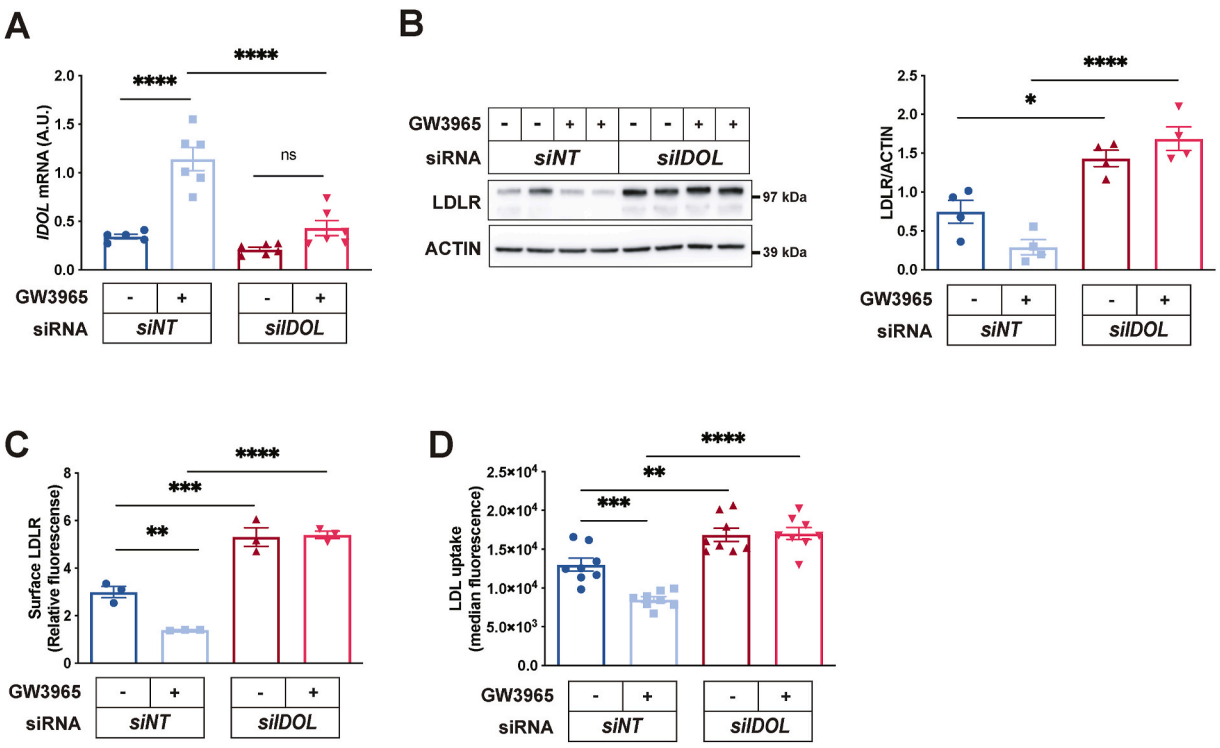

Fig. 2. IDOL-dependent regulation of LDLR level and function in enterocytes.
HCT116 cells were transfected with siRNA targeting *IDOL* (si*IDOL*) or non-targeting control (siNT). Subsequently, cells were cultured in sterol-depleted medium for 24 h and treated with 2 μM GW3965 or vehicle control as shown. (A) *IDOL* expression was determined by qPCR. (B) Total cell lysates were prepared from cells and immunoblotted and quantified as indicated. (C) LDLR on the cell surface and (D) 488-Dylight-labelled LDL uptake were determined by FACS in cells treated as indicated. Each bar and error are the mean ± SEM. Statistical differences between groups were evaluated with a one way ANOVA as described in the Materials and methods section * $p < 0.05$, ** $p < 0.01$, *** $p < 0.001$, **** $p < 0.0001$.

AMC) in DMEM supplemented with 0,5% (w/v) BSA at 37 °C. Cells were then washed twice in cold PBS, detached using TrypLE (ThermoFischer), and taken up in PBS containing 2 mM EDTA and 0.5% (w/v) BSA. Cells were subjected to flow cytometry on a Beckman Coulter CytoFLEX machine. Viable, single cells were gated, and Dylight-488-LDL signal was measured in the FITC-channel. Cells incubated in DMEM supplemented with 0,5% (w/v) BSA in the absence of labelled LDL were used for background subtraction.

2.7. Animal experiments

Male wild type C57BL6/N mice (n = 5) were treated for 4.5 days with 40 mg/kg/day GW3965 (Axon MedChem, Axon 1266) or vehicle (0.5% methylcellulose) administered by oral gavage twice a day. Following the final dose, mice were fasted for 4 h prior to euthanasia by injection anesthesia followed by cervical dislocation. The intestines were isolated and flushed with PBS. The top (duodenum), middle (jejunum) and lower (ileum) thirds of the small intestine and the colon were snap frozen in liquid nitrogen and stored at −80 °C until further processing.

The generation of *Idol*$^{(-/-)}$ mice (a kind gift from Dr Peter Tontonoz, UCLA) was previously described [42]. Control wild type C57BL6/N mice were obtained from heterozygous breeding couples. To collect tissues, age-matched adult male mice (12–20 weeks old) were fasted for 4 h and then euthanized by anesthesia injection followed by cervical dislocation. The intestinal content was flushed and emptied with PBS and the intestinal tube cut open lengthwise. To isolate enterocytes, the excised middle (jejunum) and lower (ileum) thirds of the small intestine were incubated in 20 mL PBS containing 5 mM EDTA and 1 mM DTT at 37 °C for 20 min, whereas for the colon this incubation was prolonged to 45 min. To dissociate enterocytes, samples were gently hand shaken, strained through a 100 μm cell strainer (Corning) and spun down for 5 min at 1500 rpm. The cell pellet was lysed and processed as described above under immunoblotting.

To study TICE, adult (11–14 weeks) male *Idol*$^{(-/-)}$ (N = 8, KO) and wild type control (N = 7, WT) mice received 10 mg/kg ezetimibe per day through food for two weeks. During the final 24 h, mice were housed individually and feces collected and frozen dried overnight, after which 50 mg of each faecal sample was saponified in an alcoholic KOH solution (90% EtOH, 2% KOH (w/v)) for 2 h at 70 °C. Subsequently, 500 μL H_2O and 2 mL *n*-hexane was added, followed by mixing. Samples were incubated at room temperature for 15 min, and subsequently phase separation was achieved by a 5 min centrifugation at 3000 rpm. The upper phase was collected. The lower phase was extracted again by addition of 2 mL *n*-hexane. The supernatants were pooled for each mouse and dried by evaporation under N_2. The pellet was dissolved in 250 μL H_2O supplemented with 1% Triton. Faecal sterol content was determined as described below. All the experiments received approval from the Institutional Ethical Committee on Animal Experimentation of the Academic Medical Center and adhere to national guidelines.

2.8. GC-MS analysis of fecal sterols

To 50 mg lyophilized grounded feces, 100 μL of an internal standard of 3 mM 5a-cholestane was added prior to saponification and lipid extraction as above. GC-MS was performed at the core facility of the AMC. Briefly, the pellet was dissolved in 300 μL of BSTFA (+1% TMCS) and incubated for 30 min at 80 °C. The volume of the resulting trimethylsilyl (TMS)-ethers of the sterols injected on a GC system (CPSil5 column, Agilent GC 7890B) and FID detection for quantification was 1 μL. To confirm the identity of sterols, GC-MS, including separation on an Agilent GC 7890B and subsequent selected ion monitoring of the TMS derivatives on an MSD5977A MS detector in the EI^+-mode, was performed.

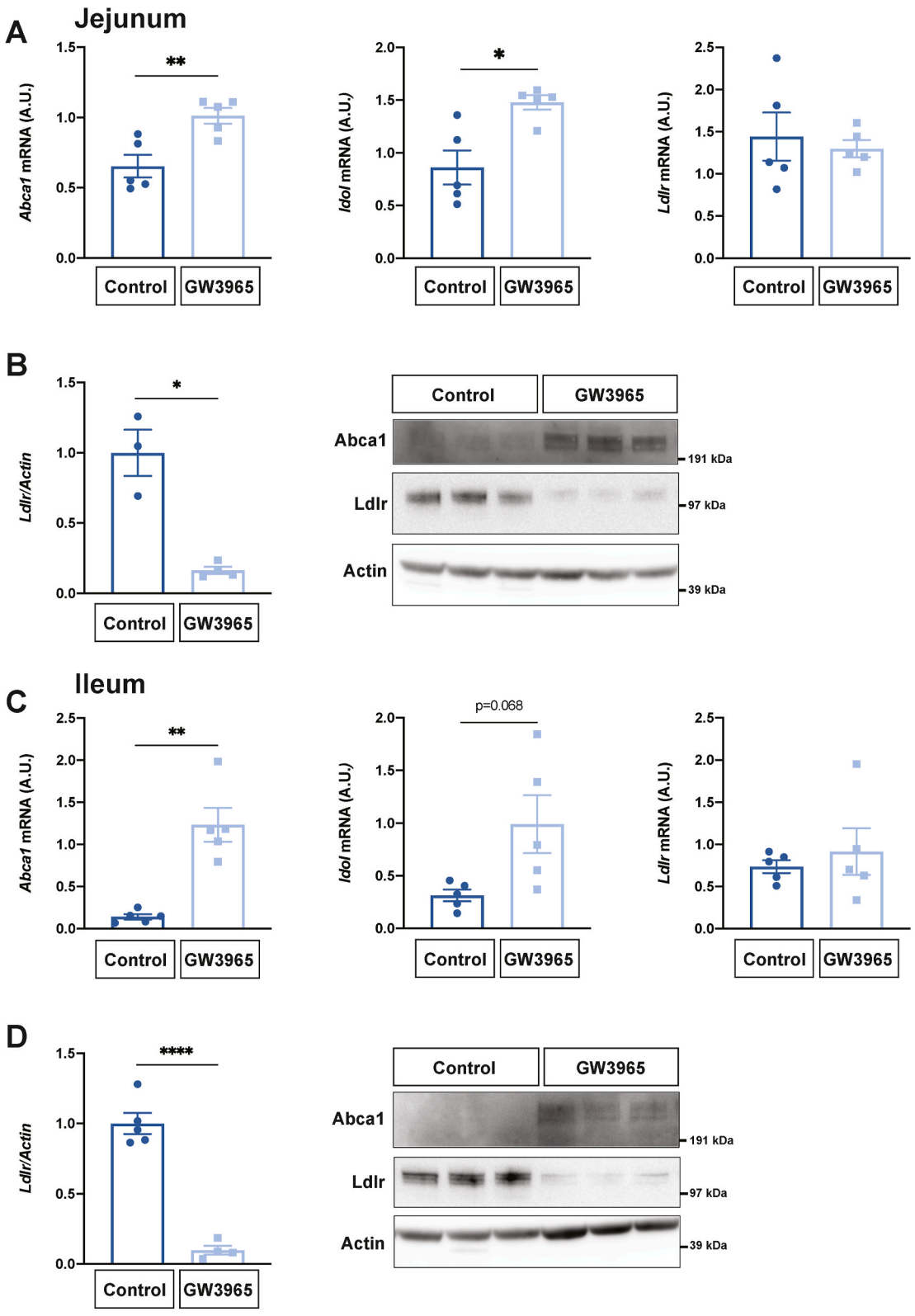

Fig. 3. Induction of intestinal *Idol* by LXR activation decreases the LDLR *in vivo*.
Wild type mice were treated with the LXR agonist GW3965 or vehicle control by oral gavage twice daily for 4.5 days, after which segments of the intestines were collected. (A) Expression of the indicated genes, and (B) proteins in the jejunum was analyzed. (C) Expression of the indicated genes, and (D) proteins in the ileum was analyzed. Each bar and error represent the mean ± SEM. Statistical differences between groups were evaluated with a Student t-test as described in the Materials and methods section * $p < 0.05$, ** $p < 0.01$, **** $p < 0.0001$.

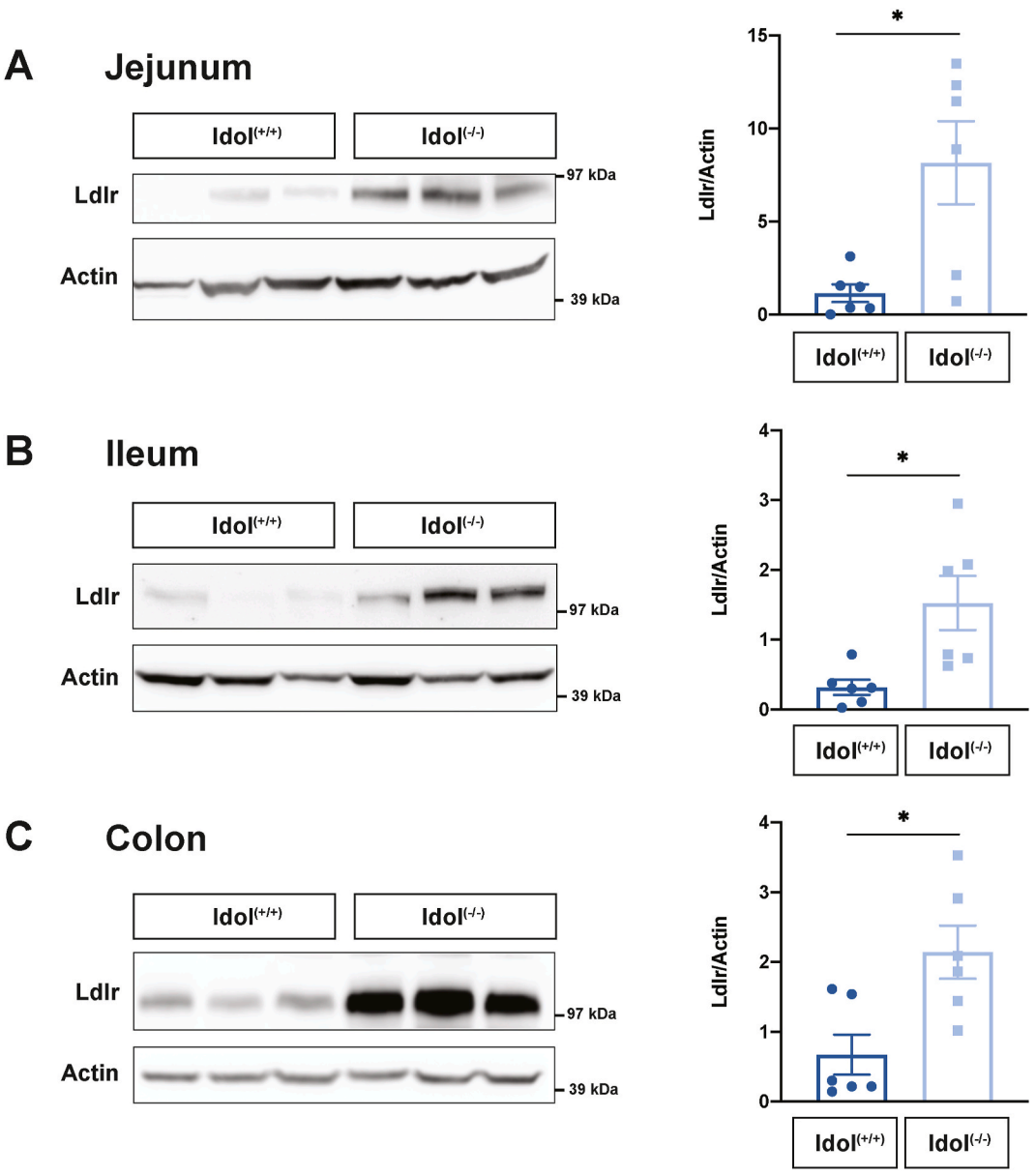

Fig. 4. Increased LDLR in primary enterocytes lacking *Idol*.
Enterocytes were isolated from the (A) jejunum, (B) ileum, and (C) colon of *Idol*$^{(-/-)}$ and their littermate wild type controls (*Idol*$^{(+/+)}$). Total tissue lysates were prepared and analyzed by immunoblotting as indicated. Each bar and error represent the mean ± SEM. Statistical differences between groups were evaluated with a Student t-test as described in the Materials and methods section * $p < 0.05$.

2.9. Statistics

Statistical significance was tested using ANOVA with Holm-Sidak *post hoc* analysis, *t*-test or *t*-test with Welch correction. When the assumption of normality was violated, Kruskal-Wallis with Dunn's multiple comparison test was employed as an alternative to the ANOVA and Mann Whitney as alternative to the *t*-test. Outliers were identified using a ROUT analysis. Prism v8 software was used for statistical analyses and $p < 0.05$ was considered significant.

3. Results

To evaluate whether the LXR-IDOL-LDLR axis is active in enterocytes, we first studied three representative human-derived intestinal epithelial cell lines: HCT116, HT29, and SW480. Pharmacological activation of LXR with the agonist GW3965 strongly increased *IDOL* expression, independent of their sterol status, indicating that the LXR pathway is active in these cells (Fig. 1A). As anticipated, sterol-depletion of these cells markedly induced the expression of the SREBP targets *HMGCR* and *LDLR* (Fig. 1B and C). Expression of *PCKS9,* a post-transcriptional regulator of the LDLR and an SREBP target, was low in all 3 cell lines (~2–10% of that measured in the hepatocyte-like cell line HepG2), and was similarly induced by sterol depletion (Supplementary Fig. 1A and B). Overall, GW3965 had a limited effect on expression of these SREBP targets, and the slight cell- and gene-specific increase observed in their expression likely represents a homeostatic response to LXR activation. In line with increased *LDLR* expression, sterol depletion of these cells led to a marked increase in the level

of LDLR protein (Fig. 1D). Importantly, activation of LXR in this setting reduced the abundance of LDLR (Fig. 1D and E).

To establish that the reduction in LDLR abundance is dependent on LXR-stimulated *IDOL* transcription, we silenced *IDOL* expression using siRNAs. Effective silencing of *IDOL* expression markedly blunted the GW3965-induced expression of *IDOL* (Fig. 2A). As a consequence of

IDOL silencing, the basal level, as well as the GW3965 stimulated levels of LDLR protein, was markedly increased (Fig. 2B). Functionally, the effect of *IDOL* silencing on total LDLR protein was recapitulated by the level of cell surface LDLR occupancy (Fig. 2C), and by the ability of cells to take up LDL via the LDLR pathway (Fig. 2D). These results establish that LXR-dependent regulation of the LDLR in the studied intestinal cell lines requires IDOL.

To evaluate whether our findings in human-derived cell lines are physiologically relevant, we first tested whether pharmacological dosing of wild type C57BL6 mice with GW3965 regulates expression of *Idol* along the intestinal tract. Similar to our findings in cell lines, we measured a strong increase in expression of *Abca1,* a canonical LXR-regulated gene, and of *Idol* by LXR activation across the whole intestinal track (Fig. 3A and C and Supplementary Fig. 2A and B). The increase in *Idol* expression was mirrored by a decrease in Ldlr protein, corroborating our *in vitro* results (Fig. 3B and D). Expression of *Pcsk9* following GW3965 treatment was comparable in the ileum and colon of these mice (Supplementary Figure 2C). We now asked the reciprocal question: does loss of *Idol* increase Ldlr protein in the intestine? To address this, we isolated primary enterocytes from distinct regions in the intestine and evaluated the level of Ldlr. Loss of *Idol* in the jejunum, ileum and colon was associated with an increase in Ldlr abundance in the isolated primary enterocytes (Fig. 4A–C), in the absence of a change in *Ldlr* or *Pcsk9* expression (Supplementary Fig. 3A-C). Collectively, this set of experiments support the notion that the LXR-IDOL-LDLR pathway is intact in enterocytes.

metabolism [26,28,29,44]. Here, we extend these initial studies and explore the physiological role of IDOL in enterocytes. As such, the most important finding of our study is the demonstration that the LXR-IDOL-LDLR axis is intact in enterocytes and that IDOL is a physiological regulator of LDLR in the gut.

In this study, we show that in a series of human intestinal cell lines and in murine primary enterocytes, IDOL/Idol governs the abundance of LDLR. In this capacity, IDOL activity is part of a homeostatic transcriptional network geared at maintaining the sterol balance in enterocytes [22]. Accordingly, treatments that reduce cellular sterol levels like sterol depletion or blocking cholesterol uptake via NPC1L1 [22] decrease LXR signaling and IDOL expression and concomitantly increase SREBP signaling [45,46]. In this setting, the combined effect of this transcriptional shift is, amongst others, an increase in LDLR protein abundance. However, we point out that our results clearly indicate that IDOL plays a homeostatic role in governing the LDLR, as the absence or silencing of *IDOL* increases the level of LDLR in enterocytes. Moreover, even with ezetimibe treatment, abundance of Ldlr remained higher in the ileum of $Idol^{(-/-)}$ mice.

The physiological significance of LDLR regulation by IDOL in enterocytes, and of LDLR in these cells is still unclear. Enterocyte-specific ablation of *Idol* in mice, despite controlling the Ldlr as we show here, had no effect on body weight [29]. Cholesterol levels in these mice were not reported, and therefore it remains unknown whether enterocyte specific *Idol* ablation affects systemic cholesterol metabolism in mice. However, we have previously shown that after 5 or 21 weeks of

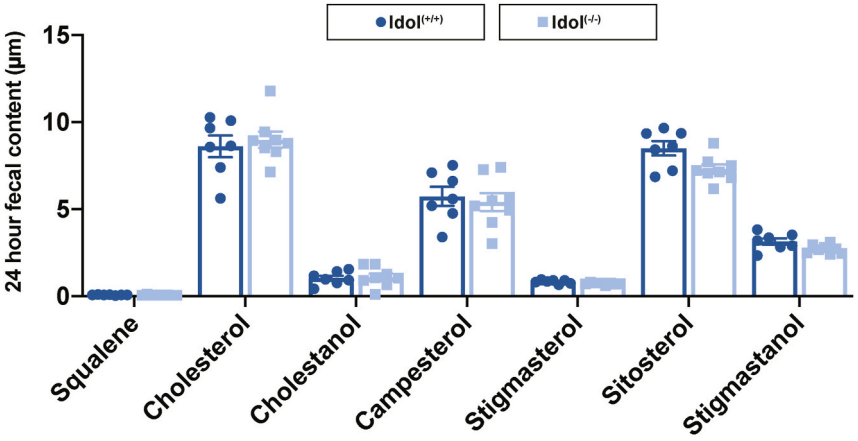

Fig. 5. Ezetimibe-induced TICE is unchanged in $Idol^{(-/-)}$mice.
$Idol^{(-/-)}$ (N = 8) and wild type controls ($Idol^{(+/+)}$, N = 7) were treated with 10 mg/kg ezetimibe for two weeks. 24-hour feces was collected per mouse and fecal sterols were extracted. The indicated sterol species were measured by GC-MS and each bar and error represent the mean ± SEM.

The nature of the lipoprotein particle and the enterocyte receptor(s) that mediate TICE is still elusive [17,43]. Therefore, to test whether *Idol*, whose ablation increases enterocyte Ldlr, plays a role in TICE, we dosed wild type and $Idol^{(-/-)}$ mice with the drug ezetimibe; an inhibitor of intestinal cholesterol absorption and a strong stimulator of TICE in mice [17,43]. Evaluation of fecal cholesterol content using a sensitive GC-MS-based assay did not reveal significant differences in 24-h fecal sterol species (Fig. 5), even though Ldlr levels in the ileum remained higher in ezetimibe-treated $Idol^{(-/-)}$ mice (Supplementary Fig. 4A and B). Collectively, our results indicate that IDOL regulates the LDLR pathway in the intestine. While we have not evaluated fecal sterols in the absence of ezetimibe, our current results do not support IDOL being a major determinant of TICE in mice.

4. Discussion

Earlier studies on the physiological roles of LXR-IDOL-LDLR have primarily focused on its role in hepatocytes and in systemic energy

western diet feeding, mice lacking *Idol* have a reduced level of circulating total cholesterol in their plasma [28]. While the global deletion of *Idol* in these mice precludes drawing strong conclusions on why cholesterol is reduced, this could suggest that either cholesterol uptake from diet is reduced, or that cholesterol loss is enhanced in $Idol^{(-/-)}$ mice. In that respect, it is interesting that we observed increased expression of hepatic *Cyp7a1*, the rate limiting enzyme in bile acid synthesis, in $Idol^{(-/-)}$ mice [28], which may also point towards alterations in bile acid metabolism in these mice.

Next to loss of cholesterol via biliary secretion, TICE has been proposed to be a major pathway for cholesterol loss in mice [17,43] and humans [8,17]. The role of LDLR in TICE is controversial [6,17]. Increasing Ldlr levels by ablation of Pcsk9 or by statin treatment have been reported to increase TICE [47], implicating involvement of the receptor. By contrast, lack of Ldlr in global *Ldlr* KO does not prevent TICE, suggesting that Ldlr is not required for this process [15,47]. It has been suggested that the constitutive ablation of *Ldlr* may induce systemic compensatory mechanisms to maintain TICE [6]. In fact, a recent

evaluation of TICE in mice with enterocyte-specific over-expression of *Ldlr* has reported increased TICE [48], which further supports a role for this receptor in TICE. Studies with intestine-specific deletion of *Ldlr* are clearly needed to understand the role of this receptor in TICE.

As several studies do support a role for LDLR in TICE [15,47,48], we reasoned that increased Ldlr in the intestine of *Idol*$^{(-/-)}$ mice, as we show, could enhance TICE. However, in contrast to studies with Pcsk9 [47], another post-transcriptional regulator of LDLR, we found no substantial effect of Idol loss on this process and fecal cholesterol content in ezetimibe-treated mice. A confounding aspect of our study was the use of global *Idol* knockout mice, as well as the fact that ezetimibe treatment in itself decreases *Idol* expression [22]. Nevertheless, Ldlr abundance was higher in the ileum of ezetimibe-treated *Idol*$^{(-/-)}$ mice, indicating that expression of activity of *Idol* is not fully abolished by this treatment. Another limitation of our study is that we did not evaluate fecal sterols in non-treated mice, which would be required for fully clarifying the role of Idol in TICE. Collectively, our findings warrant further investigation of the role of the LXR-IDOL-LDLR axis in intestinal cholesterol homeostasis and TICE. The availability of mice with intestine-specific ablation of *Idol* can facilitate these studies.

Financial support

NZ is an Established Investigator of the Dutch Heart Foundation (2013T111) and is supported by an ERC Consolidator grant (617,376), an ERC Proof-Of-Concept grant from the European Research Council (862,537) and by a Vici grant from the Netherlands Organization for Scientific Research (NWO; 016.176.643).

Author contributions

N.M.vL., S.A.E.v.W, N.Z. coneptualization of study. N.M.v.L., S.A.E. v.W., R.O., J.K.N., J.K., S.S. and M.M. performed experiments. Formal analysis and visualization was done by N.M.v.L. and S.A.E.v.W. Writing of draft, review and editing of the manuscript was done by N.M.v.L., S.A. E.v.W, and N.Z.

Declaration of competing interest

The authors declare that they have no known competing financial interests or personal relationships that could have appeared to influence the work reported in this paper.

Acknowledgements

We thank members of the Zelcer lab, Bert Groen, Irith Koster, Mart Stroobach, and Jayron Habibe for helpful discussions on this study. We thank Rudi de Waart, Fred Faz, and Wilma Smit for technical assistance.

Appendix A. Supplementary data

Supplementary data to this article can be found online at https://doi.org/10.1016/j.atherosclerosis.2020.10.898.

References

[1] S. Calandra, P. Tarugi, H.E. Speedy, a. F. Dean, S. Bertolini, C.C. Shoulders, Mechanisms and genetic determinants regulating sterol absorption, circulating LDL levels, and sterol elimination: implications for classification and disease risk, J. Lipid Res. 52 (11) (2011) 1885–1926.
[2] S. Hotta, I.L. Chaikoff, The role of the liver in the turnover of plasma cholesterol, Arch. Biochem. Biophys. 56 (1) (1955) 28–37.
[3] J.M. Dietschy, W.G. Gamel, Cholesterol synthesis in the intestine of man: regional differences and control mechanisms, J. Clin. Invest. 50 (4) (1971) 872–880.
[4] M.Y.M. van der Wulp, H.J. Verkade, A.K. Groen, Regulation of cholesterol homeostasis, Mol. Cell. Endocrinol. 368 (1–2) (2013) 1–16. Apr.
[5] M. Ouimet, T.J. Barrett, E.A. Fisher, HDL and reverse cholesterol transport: basic mechanisms and their roles in vascular health and disease, Circ. Res. 124 (10) (2019) 1505–1518. May 10.
[6] R.E. Temel, J.M. Brown, A new model of reverse cholesterol transport: enTICEing strategies to stimulate intestinal cholesterol excretion, Trends Pharmacol. Sci. 36 (7) (2015) 440–451. Jul.
[7] L. Jakulj, M.N. Vissers, CP Van Roomen, JN Van Der Veen, C.L.J. Vrins, C. Kunne, et al., Ezetimibe stimulates faecal neutral sterol excretion depending on abcg8 function in mice, FEBS Lett. 584 (16) (2010) 3625–3628.
[8] L. Jakulj, T.H. van Dijk, J.F. de Boer, R.S. Kootte, M. Schonewille, Y. Paalvast, et al., Transintestinal cholesterol transport is active in mice and humans and controls ezetimibe-induced fecal neutral sterol excretion, Cell Metabol. 24 (6) (2016) 783–794.
[9] H.C. Lifsey, R. Kaur, B.H. Thompson, L. Bennett, R.E. Temel, G.A. Graf, Stigmasterol stimulates transintestinal cholesterol excretion independent of liver X receptor activation in the small intestine, J. Nutr. Biochem. 76 (2020).
[10] T. Nakano, I. Inoue, Y. Takenaka, Y. Ikegami, N. Kotani, A. Shimada, et al., Luminal plant sterol promotes brush border membrane-to-lumen cholesterol efflux in the small intestine, J. Clin. Biochem. Nutr. 63 (2) (2018) 102–105.
[11] J.F. de Boer, M. Schonewille, M. Boesjes, H. Wolters, V.W. Bloks, T. Bos, et al., Intestinal farnesoid X receptor controls transintestinal cholesterol excretion in mice, Gastroenterology 152 (5) (2017) 1126–1138.e6. Apr.
[12] J.K. Kruit, T. Plösch, R. Havinga, R. Boverhof, P.H.E. Groot, A.K. Groen, et al., Increased fecal neutral sterol loss upon liver X receptor activation is independent of biliary sterol secretion in mice, Gastroenterology 128 (1) (2005) 147–156.
[13] JN Van Der Veen, TH Van Dijk, C.L.J. Vrins, H Van Meer, R. Havinga, K. Bijsterveld, et al., Activation of the liver X receptor stimulates trans-intestinal excretion of plasma cholesterol *□ 284 (29) (2009) 19211–19219.
[14] C.L.J. Vrins, R. Ottenhoff, K. Van Den Oever, D.R. De Waart, J.K. Kruyt, Y. Zhao, et al., Trans-intestinal cholesterol efflux is not mediated through high density lipoprotein, J. Lipid Res. 53 (10) (2012) 2017–2023.
[15] J.M. Brown, T.A. Bell, H.M. Alger, J.K. Sawyer, T.L. Smith, K. Kelley, et al., Targeted depletion of hepatic ACAT2-driven cholesterol esterification reveals a non-biliary route for fecal neutral sterol loss, J. Biol. Chem. 283 (16) (2008) 10522–10534.
[16] S.M. Marshall, A.D. Gromovsky, K.L. Kelley, M.A. Davis, M.D. Wilson, R.G. Lee, et al., Acute sterol O-acyltransferase 2 (SOAT2) knockdown rapidly mobilizes hepatic cholesterol for fecal excretion, PloS One 9 (6) (2014).
[17] J.F. de Boer, F. Kuipers, A.K. Groen, Cholesterol transport revisited: a new turbo mechanism to drive cholesterol excretion, Trends Endocrinol. Metabol. 29 (2) (2018) 123–133.
[18] F. Moreau, C. Blanchard, C. Perret, L. Flet, F. Douane, E. Frampas, et al., In vivo evidence for transintestinal cholesterol efflux in patients with complete common bile duct obstruction, J Clin Lipidol 13 (1) (2019), 213-217.e1.
[19] W.J. Simmonds, A.F. Hofmann, E. Theodor, Absorption of cholesterol from a micellar solution: intestinal perfusion studies in man, J. Clin. Invest. 46 (5) (1967) 874–890.
[20] S.H. Cheng, M.M. Stanley, Secretion of cholesterol by intestinal mucosa in patients with complete common bile duct obstruction, Exp. Biol. Med. 101 (2) (1959) 223–225. Jun 1.
[21] Y. Paalvast, J.F. de Boer, A.K. Groen, Developments in intestinal cholesterol transport and triglyceride absorption, Curr. Opin. Lipidol. 28 (3) (2017) 248–254.
[22] L.J. Engelking, M.R. McFarlane, C.K. Li, G. Liang, Blockade of cholesterol absorption by ezetimibe reveals a complex homeostatic network in enterocytes, J. Lipid Res. 53 (7) (2012) 1359–1368.
[23] V. Howe, L.J. Sharpe, S.J. Alexopoulos, S.V. Kunze, N.K. Chua, D. Li, et al., Cholesterol homeostasis: how do cells sense sterol excess? Chem. Phys. Lipids 199 (2016 Sep) 170–178, https://doi.org/10.1016/j.chemphyslip.2016.02.011.
[24] C. Hong, P. Tontonoz, Liver X receptors in lipid metabolism: opportunities for drug discovery, Nat. Rev. Drug Discov. 13 (6) (2014) 433–444.
[25] N. Zelcer, P. Tontonoz, Liver X receptors as integrators of metabolic and inflammatory signaling, J. Clin. Invest. 116 (3) (2006) 607–614. Mar 1.
[26] N. Zelcer, C. Hong, R. Boyadjian, P. Tontonoz, LXR regulates cholesterol uptake through Idol-dependent ubiquitination of the LDL receptor, Science 325 (5936) (2009) 100–104.
[27] C. Hong, S. Duit, P. Jalonen, R. Out, L. Scheer, V. Sorrentino, et al., The E3 ubiquitin ligase IDOL induces the degradation of the low density lipoprotein receptor family members VLDLR and ApoER2, J. Biol. Chem. 285 (26) (2010) 19720–19726.
[28] N.M. Van Loon, R. Ottenhoff, S. Kooijman, M. Moeton, S. Scheij, R.L.P. Roscam Abbing, et al., Inactivation of the E3 ubiquitin ligase idol attenuates diet-induced obesity and metabolic dysfunction in mice, Arterioscler. Thromb. Vasc. Biol. 38 (8) (2018) 1785–1795. Aug.
[29] S.D. Lee, C. Priest, M. Bjursell, J. Gao, D.V. Arneson, I.S. Ahn, et al., IDOL regulates systemic energy balance through control of neuronal VLDLR expression, Nat Metab 1 (11) (2019) 1089–1100.
[30] C. Hong, S.M. Marshall, A.L. McDaniel, M. Graham, J.D. Layne, L. Cai, et al., The LXR-idol axis differentially regulates plasma LDL levels in primates and mice, Cell Metabol. 20 (5) (2014) 910–918.
[31] J. Choi, J. Gao, J. Kim, C. Hong, J. Kim, P. Tontonoz, et al., The E3 ubiquitin ligase Idol controls brain LDL receptor expression, ApoE clearance, and Aβ amyloidosis, Sci. Transl. Med. 7 (314) (2015) 314ra184.
[32] J. Gao, M. Marosi, J. Choi, J.M. Achiro, S. Kim, S. Li, et al., The E3 ubiquitin ligase IDOL regulates synaptic ApoER2 levels and is important for plasticity and learning, Elife 6 (2017) 1–24.
[33] C. Hong, S. Duit, P. Jalonen, R. Out, L. Scheer, V. Sorrentino, et al., The E3 ubiquitin ligase IDOL induces the degradation of the low density lipoprotein receptor family members VLDLR and ApoER2, J. Biol. Chem. 285 (26) (2010) 19720–19726.

[34] J. Zeng, Y. Wu, Q. Liao, L. Li, X. Chen, X. Chen, Liver X receptors agonists impede hepatitis C virus infection in an Idol-dependent manner, Antivir. Res. 95 (3) (2012) 245–256.
[35] N.M. van Loon, D. Lindholm, N. Zelcer, The E3 ubiquitin ligase inducible degrader of the LDL receptor/myosin light chain interacting protein in health and disease, Curr. Opin. Lipidol. 30 (3) (2019) 192–197. Jun.
[36] T.M. Teslovich, K. Musunuru, A.V. Smith, A.C. Edmondson, I.M. Stylianou, M. Koseki, et al., Biological, clinical and population relevance of 95 loci for blood lipids, Nature 466 (7307) (2010) 707–713.
[37] V. Sorrentino, S.W. Fouchier, M.M. Motazacker, J.K. Nelson, J.C. Defesche, G. M. Dallinga-Thie, et al., Identification of a loss-of-function inducible degrader of the low-density lipoprotein receptor variant in individuals with low circulating low-density lipoprotein, Eur. Heart J. 34 (17) (2013) 1292–1297.
[38] D. Weissglas-volkov, A.C. Calkin, T. Tusie-luna, J.S. Sinsheimer, N. Zelcer, L. Riba, et al., The N342S MYLIP polymorphism is associated with high total cholesterol and increased LDL receptor degradation in humans 121 (8) (2011).
[39] D. Adi, X. Lu, Z. Fu, J. Wei, G. Baituola, Y. Meng, et al., IDOL G51S variant is associated with high blood cholesterol and increases low-density lipoprotein receptor degradation, Arterioscler. Thromb. Vasc. Biol. (2019) 1–12. December.
[40] J.M.E. Tan, E.C.L. Cook, M. van den Berg, S. Scheij, N. Zelcer, A. Loregger, Differential use of E2 ubiquitin conjugating enzymes for regulated degradation of the rate-limiting enzymes HMGCR and SQLE in cholesterol biosynthesis, Atherosclerosis 281 (2019) 137–142. October 2018.
[41] A. Loregger, J.K. Nelson, N. Zelcer, Assaying low-density-lipoprotein (LDL) uptake into cells, Methods Mol. Biol. 1583 (2017) 53–63.
[42] C. Hong, S.M. Marshall, A.L. Mcdaniel, M. Graham, J.D. Layne, L. Cai, et al., Short article the LXR – idol Axis differentially regulates plasma LDL levels in primates and mice, Cell Metabol. 20 (5) (2014) 910–918.
[43] L.F. Reeskamp, E.C.E. Meessen, A.K. Groen, Transintestinal cholesterol excretion in humans, Curr. Opin. Lipidol. 29 (1) (2018) 10–17.
[44] C. Hong, S.M. Marshall, A.L. McDaniel, M. Graham, J.D. Layne, L. Cai, et al., The LXR–Idol axis differentially regulates plasma LDL levels in primates and mice, Cell Metabol. 20 (5) (2014) 910–918.
[45] A. Moschetta, Nuclear receptors and cholesterol metabolism in the intestine, Atherosclerosis Suppl. 17 (2015) 9–11.
[46] B. Bonamassa, A. Moschetta, Atherosclerosis: lessons from LXR and the intestine, Trends Endocrinol. Metabol. 24 (3) (2013) 120–128.
[47] C. Le May, J.M. Berger, A. Lespine, B. Pillot, X. Prieur, E. Letessier, et al., Transintestinal cholesterol excretion is an active metabolic process modulated by PCSK9 and statin involving ABCB1, Arterioscler. Thromb. Vasc. Biol. 33 (7) (2013) 1484–1493. Jul.
[48] L. Meoli, D. Ben-Zvi, C. Panciotti, S. Kvas, P. Pizarro, R. Munoz, et al., Intestine-specific overexpression of LDLR enhances cholesterol excretion and induces metabolic changes in male mice, Endocrinology 160 (4) (2019) 744–758.